Hopf bifurcation of the class-*B* multimode laser

Thomas W. Carr* and Thomas Erneux†
Department of Engineering Sciences and Applied Mathematics, McCormick School of Engineering and Applied Sciences, Northwestern University, Evanston, Illinois 60208
(Received 27 December 1993)

We analyze the Risken-Nummendal–Graham-Haken instability occurring in a homogeneously broadened two-level unidirectional ring laser modeled by the Maxwell-Bloch equations. We investigate the class-*B* limit of these equations, and obtain analytically the bifurcation equation for all time-periodic traveling-wave solutions. Class-*B* lasers are characterized by slowly decaying oscillatory transients due to the small ration of population to cavity lifetimes; these include a number of practically important lasers such as CO_2, solid-state, and semiconductor lasers. We then explore the bifurcation equation and note unusual properties for the direction of bifurcation. Of particlar interest is the condition for a supercritical Hopf bifurcation that contrasts to the known subcritical bifurcation of the single-mode laser. In addition, we examine the small-wave-number limit for the Hopf bifurcation.

PACS number(s): 42.50.−p, 42.55.−f, 42.60.Mi

I. INTRODUCTION

We consider the case of a homogeneously broadened two-level unidirectional ring laser. When the laser is pumped to high inversion levels and when the cavity-mode spacing is sufficiently small, sideband modes become excited and their nonlinear interaction results in pulsations that travel around the ring geometry. This has been called the "Risken-Nummendal–Graham-Haken (RNGH)" instability after Risken and Nummendal [1,2] and Graham and Haken [3], who simultaneously derived the conditions for which deviations from the continuous-wave (cw) output become unstable. The former also carried out a numerical investigation of the self-pulsing phenomena, discussed transient effects, and determined the phase velocity of the pulsations. The instability has also been referred to as the "Rabi instability" [4], because the temporal frequency of the unstable sidebands is approximately the Rabi frequency.

Haken and Ohno [5,6] obtained an equation for the critical bifurcating mode, and found for the first time a periodic solution coexisting with the stable steady state. They discuss their result by interpreting the bifurcation equation as the negative derivative of a potential. From this they determine conditions for supercritical or subcritical Hopf bifurcations. However, because of the complexity of the coefficients appearing in their bifurcation equation, they do not determine the critical dependence on the wave number of the traveling wave, which we will show below.

Using a combination of analytical and numerical techniques, Fu [7] has specifically analyzed the traveling-wave solution in the case when the ratio of population to polarization lifetimes is small. He derives a bifurcation equation and an expression for the phase velocity, and discusses conditions for a supercritical or subcritical bifurcation, which are simpler than those described in Refs. [5,6].

In this paper, we reexamine the RNGH in the class-*B* limit. We derive the bifurcation equation and determine the direction of bifurcation analytically. We find that the bifurcation is supercritical (subcritical) for all wave numbers greater than (less than) that characterizing the minimum of the neutral stability curve. Supercritical bifurcation suggests that stable small-amplitude solutions can be observed. This contrasts with the known subcritical bifurcation of the single-mode laser modeled by the laser-Lorenz equations [8,9]. We also examine the first bifurcating traveling wave in the singular limit of small wave number. In this limit, the multimode laser equations reduce to the well-known laser-Lorenz equations.

This paper is organized as follows: In Sec. II, the multimode laser equations are reformulated as a weakly perturbed conservative system. Section III summarizes the results of the linear stability analysis. Section IV derives the leading approximation of the bifurcation equation and examines the small-amplitude limit. This is continued in Sec. V, where the vertical bifurcation occurring near the minimum of the neutral stability curve is resolved by a higher order analysis. In Sec. VI we study the limit of small wave number. Finally, Sec. VII summarizes the results.

II. FORMULATION

Risken and Nummendal [1] have normalized the Maxwell-Bloch equations so that the uniform steady-state solution (cw solution) is unity. Their equations are in terms of the real amplitudes of the electric field E, the po-

*Present address: Naval Research Laboratory, Code 6700.3, Special Project in Nonlinear Science, Washington, D.C. 20375-5000.
†Present address: Optique Nonlinéaire Théorique, ULB, Campus Plaine CP 231, Bld. du Triomphe, B-1050 Brussels, Belgium.

larization field P, and the population inversion D (subscripts indicate partial derivatives):

$$E_t+cE_r+\kappa E=\kappa P \ , \tag{1}$$

$$P_t+\gamma_\perp P=\gamma_\perp ED \ , \tag{2}$$

$$D_t+\gamma_\parallel D=\gamma_\parallel(\lambda+1-\lambda EP) \ , \tag{3}$$

$$E(r+L,t)=E(r,t) \ , \quad P(r+L,t)=P(r,t) \ ,$$

$$D(r+L,t)=D(r,t) \ . \tag{4}$$

In these equations L is the length of the laser cavity, t is time, and r is space measured in the direction of light propagation. $\gamma_\parallel$, $\gamma_\perp$, and κ are the decay constants for the population inversion, polarization, and cavity, respectively, and c is the speed of light in the host material. λ is the bifurcation parameter and measures the strength of the pumping. It is defined as

$$\lambda=\frac{D_0}{D_{\rm cw}}-1 \ , \tag{5}$$

where $D_{\rm cw}$ denotes the steady-state uniform value of the population inversion and D_0 is the pump rate.

We now rescale (1)–(4) into a form that is more suitable for our asymptotic analysis of the class-*B* limit. This corresponds to the limit $\epsilon\to 0$, where ϵ is given by

$$\epsilon=\left[\frac{\gamma_\parallel}{\kappa}\right]^{1/2}\ll 1 \ . \tag{6}$$

This is a singular limit since the problem loses one equation if $\epsilon=0$. If ϵ is too small, numerical solutions are difficult because the equations are stiff and thus require long computational times, while regular perturbation methods fail because they cannot describe the relaxation oscillations that appear for even small amplitudes.

Using singular perturbation techniques we may eliminate these difficulties by introducing new variables defined by

$$E^2=1+y \ , \tag{7}$$

$$D=1+\epsilon\left[\frac{\lambda}{2}\right]^{1/2}x \ , \tag{8}$$

$$\frac{P}{E}=1+\epsilon\left[\frac{\lambda}{2}\right]^{1/2}z \ , \tag{9}$$

$$t=\frac{1}{\epsilon\kappa\sqrt{2\lambda}}s \ , \quad r=\frac{1}{\epsilon\kappa\sqrt{2\lambda}}\frac{c}{a}\xi \ . \tag{10}$$

The new dependent variables are deviations from the cw solution. Note that the deviations for D and P/E are small but the deviation in the intensity is ~ 1. Consequently, the laser is highly sensitive to variations in the population inversion and the polarization. The rescaling allows us to treat all the dependent variables as $O(1)$ quantities and is instrumental in the success of our analysis. These new variables are motivated by the $\epsilon\to 0$ limit of the linear stability results of [1] (see Carr [10]).

After inserting (7)–(10) into (1)–(4), we obtain a weakly perturbed conservative system of equations similar to those studied by Erneux, Baer, and Mandel [11]:

$$x_s=-y-\frac{\epsilon}{\delta}[x+I_0(1+y)z] \ , \tag{11}$$

$$y_s+ay_\xi=(1+y)z \ , \tag{12}$$

$$z_s=\frac{1}{\epsilon\delta}\left[d(x-z)-y_s\frac{\left[1+\epsilon\frac{\delta}{2}z\right]}{(1+y)}\right] \ , \tag{13}$$

where the parameters d, δ, and I_0 are defined by

$$d=\frac{\gamma_\perp}{\kappa} \ , \quad \delta=\sqrt{2I_0} \ , \quad I_0=\lambda \ . \tag{14}$$

a is defined as the wave number whose value is restricted by the periodic boundary conditions. The variable ξ is a nondimensional space variable that without loss of generality we allow to vary between 0 and 2π. Thus we have 2π periodic boundary conditions of the form

$$x(\xi+2\pi,s)=x(\xi,s) \ ,$$

$$y(\xi+2\pi,s)=y(\xi,s) \ , \tag{15}$$

$$z(\xi+2\pi,s)=z(\xi,s) \ .$$

These conditions imply that the wave number a takes only discrete values; from the relation $\xi=(\epsilon\delta\kappa La)/c=2\pi n$ we have

$$a=\frac{2\pi c}{\epsilon\kappa\delta L}n \quad (n=0,\pm 1,\pm 2,\ldots) \ . \tag{16}$$

The multimode laser equations given by (11)–(15) are now in a form that is convenient for the ϵ small asymptotic limit.

III. LINEAR STABILITY ANALYSIS

In this section, we briefly redo the linear stability analysis of Risken and Nummendal [1], but in terms of the new variables x, y, and z and using a perturbation expansion valid for small ϵ. This analysis will then motivate the nonlinear analysis given in Sec. IV.

Equations (11)–(13) are linearized and we seek a solution of the form

$$\begin{bmatrix}x(\xi,s)\\ y(\xi,s)\\ z(\xi,s)\end{bmatrix}=\begin{bmatrix}u\\ v\\ w\end{bmatrix}e^{(i\xi+\sigma s)} \ . \tag{17}$$

The variables u, v, and w, as well as the growth rate σ are expanded as power series in ϵ.

From the $O(1)$ problem we find that

$$\left[1+\frac{1}{d}\right]\sigma_0^2+ia\sigma_0+1=0 \ . \tag{18}$$

Equation (18) provides a relationship between σ_0 and a. An analysis of this equation indicates that the only solution satisfies $\mathrm{Re}(\sigma_0)=0$.

From the $O(\epsilon)$ problem we determine the condition

$$\left[\frac{\sigma_0^4}{d^2}2I_0+\frac{\sigma_0^2}{d}3I_0+1+I_0\right]\frac{1}{\sqrt{2I_0}} = \left[-1+\sigma_0^2\left[1+\frac{1}{d}\right]\right]\sigma_1 . \quad (19)$$

Introducing $\sigma_0=i\omega$ into (18) and (19), we find

$$\left[1+\frac{1}{d}\right]\omega^2+a\omega-1=0 , \quad (20)$$

$$\left[\frac{\omega^4}{d^2}2I_0-\frac{\omega^2}{d}3I_0+1+I_0\right]\frac{1}{\sqrt{2I_0}} = -\left[1+\omega^2\left[1+\frac{1}{d}\right]\right]\sigma_1 . \quad (21)$$

Equation (20) is the linear dispersion relation between ω and a. Inserting $\sigma_1=\sigma_R+i\sigma_I$ into (21), we see that $\sigma_I=0$, and the condition for neutral stability ($\sigma_R=0$) leads to an expression for ω^2:

$$\omega^2=\frac{3d}{4}\pm\frac{d}{4}\left[\frac{I_0-8}{I_0}\right]^{1/2} . \quad (22)$$

We have verified that (22) is identical to the result obtained by Risken and Nummendal [1] with $\gamma\to 0$ [consider Eq. (3.9) in [1] with $\gamma_\parallel\to 0$ and $\lambda=I_0$, and substitute $\beta_i^2=\gamma_\parallel=2I_0\omega_2$; we then obtain (22) to first approximation].

Using ω as a parameter, we can determine the neutral stability curve $I_0=I_0(a)$. The neutral stability curve separates the values of I_0 corresponding to a stable basic solution from the values of I_0 for which the steady state is unstable. This curve is shown in Fig. 1 for different values of d. The minimum of the curve is given by

$$I_0=I_m=8 , \quad \omega=\omega_m=\pm\sqrt{3d/4} , \quad a=a_m=\frac{(1-3d)}{4\omega_m} . \quad (23)$$

The critical value of I_0 above which the uniform steady state is unstable corresponds to $I_0=\min[I_0(a)]$, where $a=a(n)$ $n=(0,1,2,\ldots)$ admits discrete values given by (15).

Since I_0 must remain positive we see from (21) that $\omega^2\in(d/2,d)$, and then from (20) that

$$a\in\left[\frac{d^{1/2}}{\sqrt{2}}\left[1-\frac{1}{d}\right] , \ d^{1/2}\right] . \quad (24)$$

This is in contrast to most other systems in which the neutral stability curve exists for all values of the wave number. Here the unstable wave numbers are confined within a fixed band for all values of I_0. As $d\to\infty$ the bandwidth of the neutral stability curve is $O(d^{1/2})$.

For $d>\frac{1}{3}$, the minimum wave number a_m is positive, while ω_m is negative (solid lines in Fig. 1). The dashed curve is for $\omega_m>0$, $a_m<0$, and is the neutral stability curve for the complex-conjugate solution. Both represent a wave traveling in the positive direction, and it is sufficient to discuss only one of the curves. I_m is independent of the parameter d, but the minimum wave number is $O(d^{1/2})$ as $d\to\infty$. From Fig. 1, we see that for $d=\frac{1}{3}$ the minimum wave number is identically zero; in this case, the original system reduces to a set of ordinary differential equations. For $d<\frac{1}{3}$, the minimum of the solid neutral stability curve moves to the left-hand plane, indicating that the waves switch direction.

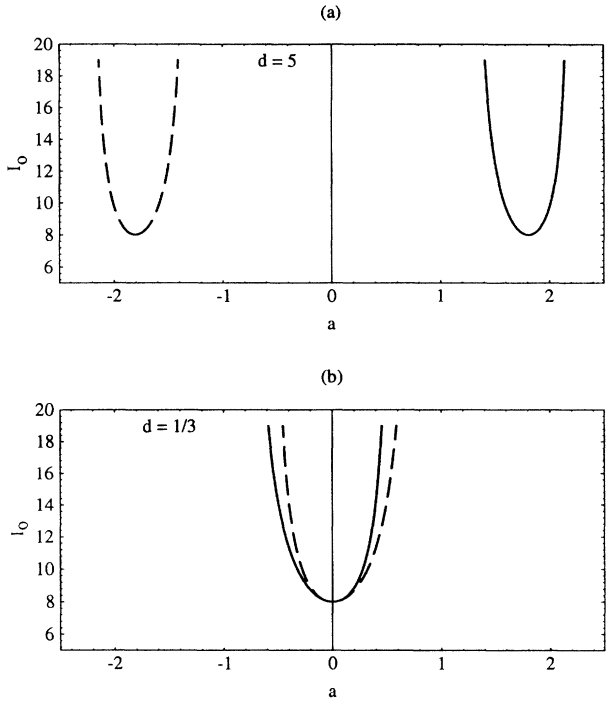

FIG. 1. Neutral stability curve, where I_0 is the bifurcation parameter and a is the wave number for (a) $d=5$ and (b) $d=\frac{1}{3}$. Note that in (b) the minimum wave number is zero, indicating no spatial variation. As $d\to\infty$ the minimum of the curve and the width both scale as $O(d^{1/2})$. Further, the curves do not extend to all a; a is bound to the region $[(d/2)^{1/2}(1-1/d),d^{1/2}]$.

The $d\to\infty$ limit of the Maxwell-Bloch equations (1)–(4) is interesting because it may reduce the three-variable system to two rate equations. However, this limit is not obvious because $a_m\to\infty$ as $d\to\infty$, and is another source of singularity distinct from $\epsilon\to 0$.

IV. NONLINEAR ANALYSIS

We now assume that the first instability of the uniform solution corresponds to a simple eigenvalue, i.e., there is a unique n such that $a(n)$ becomes unstable at $I_0(a(n))$. Double eigenvalues are possible for exceptional values of d but are not considered in the present analysis.

To analyze $O(1)$ solutions bifurcating from a simple eigenvalue, we consider the limit $\epsilon\to 0$ of the fully nonlinear system, (11)–(15). Specifically, we seek a solution of the form

$$x(\xi,s;\epsilon)\approx x_0(\xi,s)+\epsilon x_1(\xi,s)+\cdots ,$$
$$y(\xi,s;\epsilon)\approx y_0(\xi,s)+\epsilon y_1(\xi,s)+\cdots , \quad (25)$$
$$z(\xi,s;\epsilon)\approx z_0(\xi,s)+\epsilon z_1(\xi,s)+\cdots .$$

We substitute (25) into (11)–(15) and equate to zero the coefficients of each power of ϵ. The polarization variables z_0 and z_1 can be eliminated from the resulting equations leading to the following problems for (x_0,y_0) and (x_1,y_0):

$$x_{0_s}+y_0=0 , \quad (26)$$

$$(1+1/d)y_{0_s}+ay_{0\xi}=(1+y_0)x_0 , \quad (27)$$

$$x_0(\xi+2\pi,s)=x_0(\xi,s) , \quad y_0(\xi+2\pi,s)=y_0(\xi,s) , \quad (28)$$

and

$$x_{1_s}+y_1=-\frac{1}{\delta}\left[x_0(1+I_0)+I_0x_0y_0-\frac{I_0}{d}y_{0_s}\right] , \quad (29)$$

$$\left[1+\frac{1}{d}\right]y_{1_s}+ay_{1\xi}-x_1 =(x_0y_1+y_0x_1)+\frac{\delta}{d}\left[(1+y_0)y_0-\frac{1}{2d}\frac{y_{0_s}^2}{1+y_0} +\frac{1}{d}y_{0_{ss}}-\frac{1}{2}x_0y_{0_s}\right] , \quad (30)$$

$$x_1(\xi+2\pi,s)=x_1(\xi,s) , \quad y_1(\xi+2\pi,s)=y_1(\xi,s) . \quad (31)$$

We are interested in determining periodic traveling-wave solutions of these equations. Specifically, we seek 2π periodic solutions in the characteristic variable

$$Z=\xi+\omega s , \quad (32)$$

where ω is the Hopf bifurcation frequency to be determined. Introducing (32) into (26)–(28) changes the partial differential equation into two coupled ordinary differential equations (dot denotes differentiation with respect to Z). The leading-order problem becomes

$$\omega\dot{x}_0+y_0=0 ,$$
$$[(1+1/d)\omega+a]\dot{y}_0=(1+y_0)x_0 , \quad (33)$$
$$x_0(Z+2\pi)=x_0(Z) , \quad y_0(Z+2\pi)=y_0(Z) . \quad (34)$$

This new system of equations is conservative and admits a one-parameter family of periodic solutions with the first integral given by

$$C=y_0-\ln|1+y_0|+\tfrac{1}{2}\beta x_0^2 , \quad (35)$$

where C is the constant of integration and the coefficient β is defined as

$$\beta=\frac{\omega}{\left[1+\frac{1}{d}\right]\omega+a} . \quad (36)$$

By studying this system in the phase plane (x_0,y_0), we find that for each value of $C\neq 0$, there is a periodic orbit surrounding the center $(x_0,y_0)=(0,0)$ and bounded below by the line $y_0=-1$. Near the center, the orbits correspond to small-amplitude periodic solutions and are characterized by low values of C. Near the line $y_0=-1$, the periodic orbits correspond to relaxation oscillations and are characterized by large values of C, see Fig. 2. For example, we note from our phase-plane analysis that the maximum value of x_0 occurs at $y_0=0$. From (35) we then see that the maximum value of x_0 is $x_0=x_M=(2C/\beta)^{1/2}$. Thus the maximum value of x_0 is proportional to $C^{1/2}$. By comparing Fig. 2(b) to the numerical results of Risken and Nummendal [1], we see that the dynamics of the conservative system model the pulsating behavior very well.

We would like to know how the amplitude of the periodic solution x_M (or equivalently C) and the frequency vary as a function of the bifurcation parameter, I_0. This is accomplished by using the fact that the period is equal to 2π and analyzing the higher-order problem. Introducing (32) and (33) into the $O(\epsilon)$ problem, we obtain

$$\omega\dot{x}_1+y_1=-\frac{1}{\delta}\left[x_0(1+I_0)+I_0x_0y_0-\frac{I_0}{d}y_{0_s}\right] ,$$
$$\left[\left[1+\frac{1}{d}\right]\omega+a\right]\dot{y}_1-x_1 =(x_0y_1+y_0x_1)+\frac{\delta}{d}\left[(1+y_0)y_0-\frac{1}{d}\frac{y_{0_s}^2}{1+y_0} +\frac{1}{d}y_{0_{ss}}-\tfrac{1}{2}x_0y_{0_s}\right] , \quad (37)$$

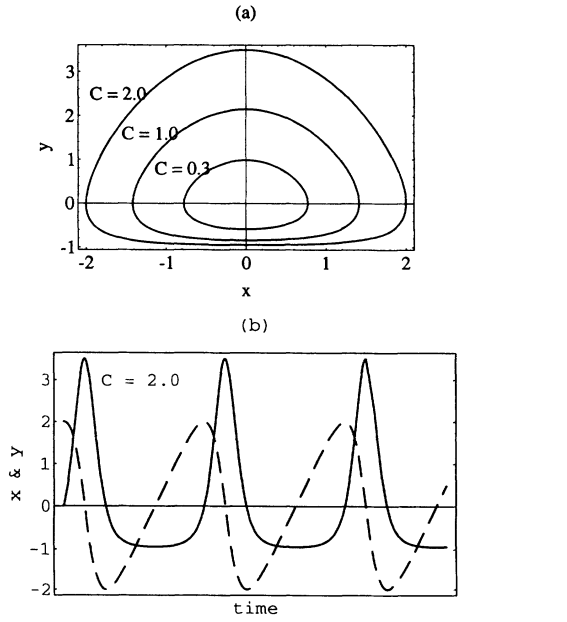

FIG. 2. x is the population inversion and y is the intensity of the $O(1)$ Eq. (33). (a) Phase-space plot, y vs x for $\beta=1$. The orbits are bound below by the invariant line $y=-1$. (b) The temporal evolution of x (dashed) and y (solid), showing relaxation oscillations for $C=2$.

$$x_1(Z+2\pi)=x_1(Z)\ ,\quad y_1(Z+2\pi)=y_1(Z)\ . \tag{38}$$

Since the homogeneous problem admits a periodic solution, namely, $(x_{1_h},y_{1_h})=(x_{0Z},y_{0Z})$, the right-hand side must satisfy a solvability condition. This requires the solution to the homogeneous adjoint problem given by

$$\begin{aligned} -\omega\dot{x}_a&=\beta(1+y_0)y_a\ ,\\ -\omega\dot{y}_a&=-x_a-\beta x_0 y_a\ , \end{aligned} \tag{39}$$

and its solution is

$$x_a=x_0\ ,\quad y_a=\frac{y_0}{\beta(1+y_0)}\ . \tag{40}$$

The solvability condition can be written as

$$\left\{-\left[1+I_0\left[1-\frac{\beta}{d}\right]\right]+\frac{2}{d}I_0\beta\left[1-\frac{\beta}{d}\right]\right\}\int_0^{2\pi/\omega}x_0^2dZ=0\ , \tag{41}$$

where the following equalities have been used to simplify the result (see the Appendix):

$$\begin{aligned} &\int_0^{2\pi/\omega}x_0^2y_0dZ=0\ ,\\ &\int_0^{2\pi/\omega}y_0^2dZ=\beta\int_0^{2\pi/\omega}x_0^2dZ\ . \end{aligned} \tag{42}$$

Since the integral is always positive, its coefficient must be equal to zero. This leads to an elegant expression for I_0:

$$I_0=\frac{\left[a+\left[1+\frac{1}{d}\right]\omega\right]^2}{(a+\omega)\left[-a-\left[1-\frac{1}{d}\right]\omega\right]}\ . \tag{43}$$

This equation represents the amplitude or bifurcation equation.

It was first determined by Fu [7]. He found this expression by determining numerically the second relation in (42). The bifurcation equation relates the frequency ω to the bifurcation parameter I_0. Together with the 2π periodicity condition, which provides a relation between ω and the amplitude of the periodic solution, we may determine how the amplitude changes with I_0. In general, this 2π periodicity condition cannot be found analytically.

However, in the limit of small amplitude we can determine an analytical approximation for the amplitude dependence of the frequency. We can then determine the bifurcation parameter as a function of the amplitude by substituting into (43). We now summarize the results.

We start by determining a small-amplitude periodic solution of the $O(1)$ solution by using the Poincaré-Lindstedt method [12], where we define the small parameter α as

$$\alpha^2=\int_0^{2\pi/\omega}|x_0|^2dZ\ll 1\ . \tag{44}$$

x_0, y_0, and ω are expanded as power series in α. We then solve the problems that result from setting the coefficient of each power of α to zero. From solvability conditions we can determine ω out to $O(\alpha^2)$.

Having determined the frequency, we substitute into the bifurcation equation (43) to obtain

$$I_0=I_H+\alpha^2I_H^2\omega_0^4\frac{4}{3d^2}\frac{1-\left[1+\frac{1}{d}\right]\omega_0^2}{1+\left[1+\frac{1}{d}\right]\omega_0^2}\left[\frac{3d}{4}-\omega_0^2\right]\ , \tag{45}$$

where I_H is defined as the Hopf bifurcation point and is given by

$$I_H=\frac{1}{\left[\frac{2}{d}\omega_0^2-1\right]\left[1-\frac{1}{d}\omega_0^2\right]}\ , \tag{46}$$

and ω_0 is

$$\left[1+\frac{1}{d}\right]\omega_0^2+a\omega_0-1=0\ . \tag{47}$$

The deviation $I_0=I_H$ is quadratic in α, so that depending on the value of ω_0, the bifurcation may be supercritical or subcritical. We find that the quantity $[1-(1+1/d)\omega_0^2]$ is negative. Thus, when $a>a_m$ ($a<a_m$), then $\omega_0^2>3d/4$ ($\omega_0<3d/4$), and the bifurcation is supercritical (subcritical). Stability (instability) of the supercritical (subcritical) bifurcation is found from the original equations, (1)–(4). If the most unstable wave number lies at the minimum of the neutral stability curve, $a=a_m$, then $\omega_2=3d/4$ and the coefficient of the α^2 term in the bifurcation equation is zero. This is referred to as a vertical bifurcation and is a new singularity in the problem. Because this vertical bifurcation is located exactly at the minimum of the neutral stability curve, and thus corresponds to the most unstable wave number, it is important to resolve this singularity. This is accomplished by a higher-order analysis described in Sec. V.

V. RESOLUTION OF THE VERTICAL BIFURCATION

Our purpose is to determine the bifurcation diagram at and near $a=a_m$. To this end, we define a new small parameter $\eta\ll 1$

$$a(\eta)=a_m+\eta^2a_2\quad(a_2=\pm 1)\ , \tag{48}$$

as a measure of the detuning of the wave number from the minimum. We again employ the small-amplitude Poincaré-Lindstedt method by expanding x_0, y_0, and ω in a series in η:

$$\begin{aligned} x_0(Z;\eta)&\approx\eta x_{01}(Z)+\eta^2x_{02}(Z)+\cdots\ ,\\ y_0(Z;\eta)&\approx\eta y_{01}(Z)+\eta^2y_{02}(Z)+\cdots\ , \end{aligned} \tag{49}$$

$$\omega(\eta)\approx\omega_0+\eta^2\omega_2+\cdots\ . \tag{50}$$

After substituting (48) and (49) into (33), we find that

$$x_0 \approx \eta(\alpha e^{iZ} + \text{c.c.}) + O(\eta^2) ,$$

$$y_0 \approx \eta(-i\omega_0 \alpha e^{iZ} + \text{c.c.}) + O(\eta^2) . \quad (51)$$

An analysis of the higher-order problems fully determines the frequency correction

$$\omega_0 = \omega_m = \pm\sqrt{3d/4} , \quad (52)$$

$$\omega_2 = -\frac{d\omega}{(7+3d)}|\alpha|^2 - \frac{3d}{(7+3d)}a_2 . \quad (53)$$

Note that ω_2 depends on the amplitude α and the wave number a_2.

These results are then supplied to the bifurcation equation (43). In particular, we consider $d > \frac{1}{3}$, $a_m > 0$, and $\omega_0 = -(3d/4)^{1/2}$, so that we are examining the positive neutral stability curve in Fig. 1. We obtain

$$\frac{I_0 - 8}{(\eta^4 72)} = m_1|\alpha|^4 + m_2 a_2|\alpha|^2 + m_3 a_2^2 , \quad (54)$$

where the coefficients m_1, m_2, and m_3 are all positive and given by

$$m_1 = \left[\frac{(3d-1)d}{4(7+3d)}\right]^2 ,$$

$$m_2 = \frac{2\sqrt{3d}\,(3d-1)d}{(7+3d)^2} ,$$

$$m_3 = \frac{48d}{(7+3d)^2} . \quad (55)$$

The left-hand side indicates that we are considering small deviations from the minimum of the neutral stability curve where $I_m = 8$. The right-hand side indicates that for positive deviations in the wave number, $a_2 > 0$, the bifurcation is supercritical and stable. At the minimum, $a_2 = 0$, the bifurcation is also supercritical and stable. For deviations in the wave number below the minimum, $a_2 < 0$, the limit point of the small-amplitude subcritical bifurcation is found. This determines a hysteresis loop in which the basic state will jump up to large-amplitude solutions at the bifurcation point and jump down to the basic state at the limit point. Note that for $d = \frac{1}{3}$ the result is again vertical, indicating another singular limit. This limit is the subject of Sec. VI. Figure 3 illustrates this discussion.

In summary, we have found a branch of stable periodic solutions that emerge from a Hopf bifurcation point ($a \geq a_m$), and a branch of stable periodic of solutions that emerge from a limit point ($a \leq a_m$). This branch may overlap a stable steady state. All these branches are of small amplitude and have been obtained by a local analysis near $a = a_m$. These bifurcation diagrams contrast with the strictly subcritical Hopf bifurcation obtained in the case of the laser-Lorenz equation (i.e., $a = 0$).

We have also determined the phase velocity of the resulting traveling wave. In terms of the original unscaled space and time variables r and t, it is given by $v = -(\omega/a)c$, where c is the velocity of light in the host material. Our asymptotic result is in agreement with that

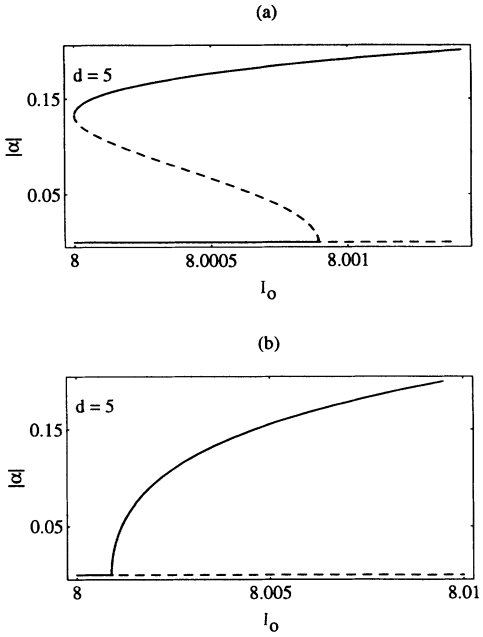

FIG. 3. (a) Subcritical Hopf bifurcation occurring when $a < a_m$. There is a jump up to periodic solutions at the bifurcation point and a jump down to the basic state at the saddle-node point characterizing hysteresis. Solutions are unstable along the dashed curves and stable along the solid curves. (b) Supercritical Hopf bifurcation occurring when $a > a_m$. Small-amplitude periodic solutions exist as soon as the pump intensity reaches the Hopf bifurcation point.

of Fu's [7] when the latter is analyzed close to the second threshold. Details are given in [10].

VI. SMALL WAVE NUMBER

In this section we examine the limit of small ($a \to 0$) wave number by examining limits $d \to \frac{1}{3}$. We call this the laser-Lorenz equation limit.

As $d \to \frac{1}{3}$, we found in Sec. V that the bifurcation equation was singular; both m_1 and m_2 in (54) approach zero in this limit. We also note from the linear stability analysis that for $d = \frac{1}{3}$ the minimum wave number is zero, $a_m(d = \frac{1}{3}) = 0$, see Fig. 1. Note that when $a = 0$, the spatial derivative no longer appears in the original equations, (12), and the system is equivalent to the laser-Lorenz equations [8,9]. We now summarize the results of our analysis.

In contrast to Sec. V, which was a local analysis about a_m, we propose to analyze the local region near $a = 0$. We then scale d such that the minimum of neutral stability curve is within this region. That is, the deviation of d from $\frac{1}{3}$ defines the new small parameter and determines a_m. We reanalyze (26)–(31) using the Poincaré-Lindstedt method where x, y, ω, a, and d are expanded in the new small parameter.

We find that there is no qualitative change in the behavior of the system; the bifurcation is supercritical (subcritical) for positive (negative) values of $a - a_m$. The range of wave numbers $a \in (0, a_m)$ for which the bifurca-

tion is subcritical approaches zero as $d \to \frac{1}{3}$. If $d = \frac{1}{3}$, the bifurcation is vertical at $a = 0$ but supercritical if $a > 0$. Note that the bifurcation of the laser-Lorenz equations is known to be subcritical [13,14]. Moreover, the $O(1)$ amplitude of the period solution is changing if $|I_0 - 8| = O(\epsilon^2)$. This result requires a higher-order analysis up to the $O(\epsilon^3)$ problem [15]. In the present analysis, we have only explored the $O(\epsilon)$ so that, if $a = 0$, the bifurcation remains vertical at this order of the perturbation analysis. It is this particular feature of the laser-Lorenz equations that explains why we have a change of the direction of bifurcation localized at $a = a_m$.

VII. DISCUSSION

We have performed a detailed analysis of the Hopf bifurcation occurring at the laser's second threshold. The success of this analysis was due to simplifications that resulted by taking advantage of the limit $\gamma_\parallel/\kappa \ll 1$. In this limit the multimode laser equations are reformulated as a weakly perturbed conservative system. The leading-order problem remains nonlinear but is now much easier to solve because the polarization can be eliminated and the resulting two-variable system is conservative. Frequency dispersion is studied in the conservative system, while the bifurcation properties are taken into account by a solvability condition determined at the $O(\epsilon)$ problem.

The direction of the bifurcation is shown to depend upon the wave number of the bifurcating mode. If the wave number is greater than (less than) that at the minimum of the neutral stability curve, a_m, then there is a supercritical bifurcation (subcritical bifurcation). The former is in contrast to the laser-Lorenz equations of the single-mode laser in which the Hopf bifurcation is known to be always subcritical. The bifurcation is singular at the minimum of the neutral stability curve requiring a higher-order perturbation analysis to fully determine the bifurcation equation. A local analysis about the minimum of the neutral stability curve resolves the vertical bifurcation and determines the limit point of the subcritical bifurcation.

In the singular limit $d \to \frac{1}{3}(a_m \to 0)$, the multimode equations become the laser-Lorenz equations. The bifurcation analysis shows that there is no qualitative change in the bifurcation properties about the minimum wave number, but that the bifurcation again becomes increasingly vertical as d gets closer to $\frac{1}{3}$. This singularity cannot be resolved with the $O(\epsilon)$ truncation of the original system.

We mention that the limit $d \to \infty (a_m \to \infty)$ is also singular. This limit is commonly used to obtain the laser-rate equations from the Maxwell-Bloch equations. While the laser-rate equations have only damped oscillations, careful analysis indicates that the Hopf bifurcation persists in this limit. Our results will be presented elsewhere.

We wish to add that a numerical analysis of (33) and (34) is found to substantiate the asymptotic results. For a fixed amplitude, a shooting method is used to determine the frequency such that when (33) is stepped forward in time, the period is 2π. The computed frequency is used in Eq. (43) to determine the bifurcation parameter I_0. By scanning through values of the amplitude, we can thus find the corresponding values of the bifurcation parameter. A comparison of the numerical versus the analytical results is shown in Fig. 4. The numerical analysis was continued to $O(1)$ values of the amplitude and there was no qualitative change from that predicted by the asymptotic analysis.

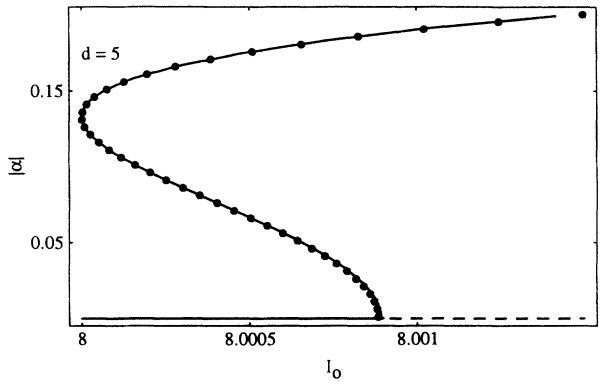

FIG. 4. Comparison of the numerical result vs analytical result for the subcritical Hopf bifurcation. The solid disks represent the numerical data while the analytical result is shown by the solid curve.

ACKNOWLEDGMENTS

This work was supported by the U.S. Air Force Office of Scientific Research under Grant No. AFSOR93-1-0084 and the National Science Foundation under Grant No. DMS9308009. This work was also supported by the Fonds National de la Recherche Scientifique (Belgium) and the Interuniversity Attraction Pole of the Belgian government.

APPENDIX: INTEGRALS OF THE $O(\epsilon)$ PROBLEM

Here we evaluate the integrals obtained when computing the solvability condition of Sec. IV. The functions x_0 and y_0 satisfy the equations

$$\omega \dot{x}_0 + y_0 = 0 , \tag{A1}$$

$$\frac{\omega}{\beta}\dot{y}_0 = (1 + y_0)x_0 , \tag{A2}$$

$$x_0(Z + 2\pi) = x_0(Z) , \quad y_0(Z + 2\pi) = y_0(Z) . \tag{A3}$$

Consider the following integral:

$$I_1 = \int_0^P x_0^2 y_0 dZ . \tag{A4}$$

Using (A1), we show that this integral is zero. Indeed, solving for dZ, (A4) can be rewritten as

$$I_1 = -\omega \int_0^P x_0^2 dx_0 = 0 \ . \tag{A5}$$

Consider the following integral:

$$I_2 = \int_0^P x_0^2 dZ \ . \tag{A6}$$

Using the fact that $I_1 = 0$, we write $I_2 = I_2 + I_1$

$$I_2 = \int_0^P x_0^2 dZ = \int_0^P x_0^2 (1 + y_0) dZ \ . \tag{A7}$$

Using (A2), we again solve for dZ and substitute into (A7) to find

$$I_2 = \frac{\omega}{\beta} \int_0^P x_0 dy_0 \ . \tag{A8}$$

Consider the following integral:

$$I_3 = \int_0^P y_0^2 dZ \ . \tag{A9}$$

Using (A1) we obtain

$$I_3 = -\omega \int_0^P y_0 dx_0 \ . \tag{A10}$$

Upon integrating by parts the result is

$$I_3 = -\omega \left[0 - \int_0^P x_0 dy_0 \right] = \omega \int_0^P x_0 dy_0 \ . \tag{A11}$$

We conclude that

$$I_3 = \beta I_2 \text{ or } \int_0^P y_0^2 dZ = \beta \int_0^P x_0^2 dZ \ . \tag{A12}$$

[1] H. Risken and K. Nummendal, J. Appl. Phys. **39**, 4662 (1968).

[2] H. Risken, in *Optical Instabilities,* edited by R. W. Boyd, M. G. Raymer, and L. N. Narducci, Cambridge Studies in Modern Optics Vol. 4 (Cambridge University Press, Cambridge, 1986), pp. 20–33.

[3] R. Graham and H. Haken, Z. Phys. **213**, 420 (1968).

[4] K. Ikeda, K. Otsuka, and K. Matsumoto, Prog. Theor. Phys. Suppl. No. **99**, 295 (1989).

[5] H. Haken and H. Ohno, Opt. Commun. **16**, 205 (1976).

[6] H. Ohno and H. Haken, Phys. Lett. **59A**, 261 (1976).

[7] H. Fu, Phys. Rev. A **40**, 1868 (1989).

[8] E. N. Lorenz, J. Atmos. Sci. **20**, 130 (1963).

[9] H. Haken, Phys. Lett. **53A**, 77 (1975).

[10] T. W. Carr, Ph.D. thesis, Northwestern University, 1993.

[11] T. Erneux, S. M. Baer, and P. Mandel, Phys. Rev. A **35**, 1165 (1987).

[12] A. Nayfeh, *Perturbation Methods* (Wiley, New York, 1973).

[13] C. Sparrow, *The Lorenz Equations: Bifurcations, Chaos, and Strange Attractors* (Springer-Verlag, New York, 1982).

[14] C. Ning and H. Haken, Phys. Rev. A **41**, 6577 (1990).

[15] S. Baer and T. Erneux (unpublished).